Science Signaling
AAAS

www.sciencesignaling.org/cgi/content/full/7/339/ra79/DC1

Supplementary Materials for

Macromolecular assembly of the adaptor SLP-65 at intracellular vesicles in resting B cells

Michael Engelke, Sona Pirkuliyeva, Julius Kühn, Leo Wong, Janina Boyken, Nadine Herrmann, Stefan Becker, Christian Griesinger, Jürgen Wienands*

*Corresponding author. E-mail: jwienan@gwdg.de

Published 19 August 2014, *Sci. Signal.* **7**, ra79 (2014)
DOI: 10.1126/scitranslmed.2005104

The PDF file includes:

fig. S1

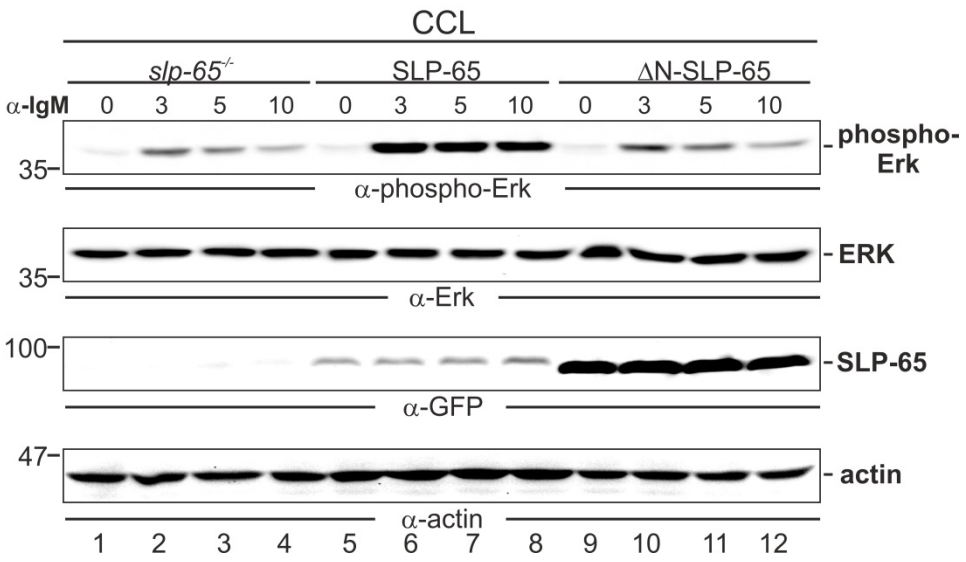

Fig. S1. The N terminus of SLP-65 is essential for the BCR-induced activation of ERK. SLP-65–deficient DT40 cells were retrovirally transduced with either empty control vector (lanes 1 to 4) or vectors encoding citrine-tagged versions of WT SLP-65 or ΔN-SLP-65 (lanes 5 to 8 and 9 to 12, respectively). Transductants were left untreated or were stimulated through their BCR with anti-IgM antibodies for the indicated times. Cleared cellular lysates (CCLs) were subjected to Western blotting analysis with antibodies against the indicated proteins. Relative molecular masses of marker proteins are indicated on the left (kD). Western blots are representative of three independent experiments.

fig. S2

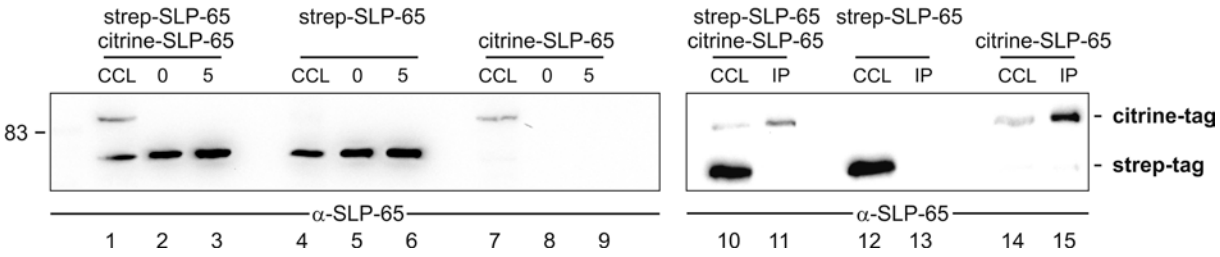

Fig. S2. Differently tagged SLP-65 forms do not coimmunoprecipitate with each other. To assess the possible multimerization of SLP-65, DT40 cells that coexpressed streptavidin-tagged and citrine-tagged versions of SLP-65 (lanes 1 to 3 and 10 to 11) or cells that expressed just one of these forms (lanes 4 to 9 and 12 to 15) were left untreated (0) or were stimulated through their BCR for 5 min (5). SLP-65 was affinity-purified by streptactin beads (left) or by immunoprecipitation (IP) with anti-GFP antibodies (right) and were analyzed together with cleared cellular lysates (CCL) Western blotting with an anti-SLP-65 antibodies. Relative molecular masses of marker proteins are indicated on the left (kD). Western blots are representative of three independent experiments.

fig. S3

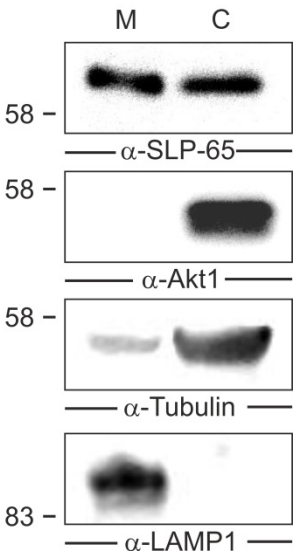

Fig. S3. SLP-65 associates with membranes in resting human B cells. Ramos cells were disrupted with a nitrogen cavitation pump (10 bar, 3 min). Post-nuclear supernatant was subjected to ultracentrifugation at 100,000*g* for 1 hour. The supernatant containing cytosolic proteins was removed and subjected to centrifugation at 100,000*g*. The membrane pellet was resuspended in 0.3% triton X-100 to extract membrane proteins. The protein concentrations of the cytosolic (C) and membranous (M) fractions were determined by BCA assay (Pierce). Samples were analyzed by Western blotting with antibodies specific for SLP-65 (top), the cytosolic markers Akt1 and tubulin (second and third panels), and the membrane-associated protein LAMP1 (bottom). Relative molecular masses of marker proteins are indicated on the left (kD). Western blots are representative of two independent experiments.

fig. S4

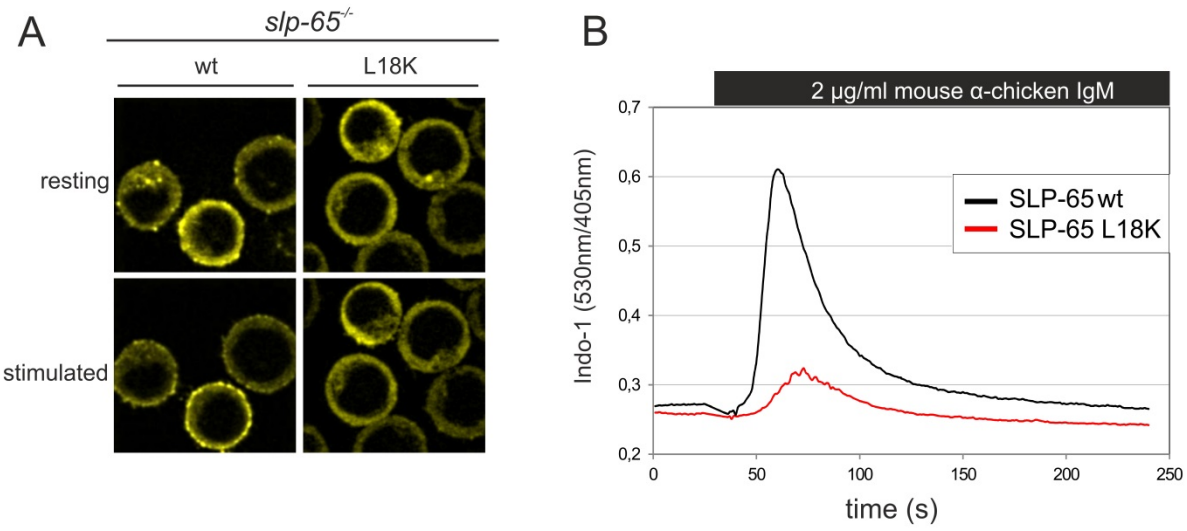

Fig. S4. The L18K variant of SLP-65 cannot signal. (**A**) Confocal microscopy analysis of *slp65*$^{-/-}$DT40 cells reconstituted with WT SLP-65 (left) or the L18K variant SLP-65 (right) before and after 3 min of BCR stimulation with anti-chicken IgM antibodies (2 µg/ml). (**B**) Ca^{2+} mobilization profiles of the cells described in (A) were determined by flow cytometric analysis of cells gated for equal amounts of citrine. Data are representative of three independent experiments.

fig. S5

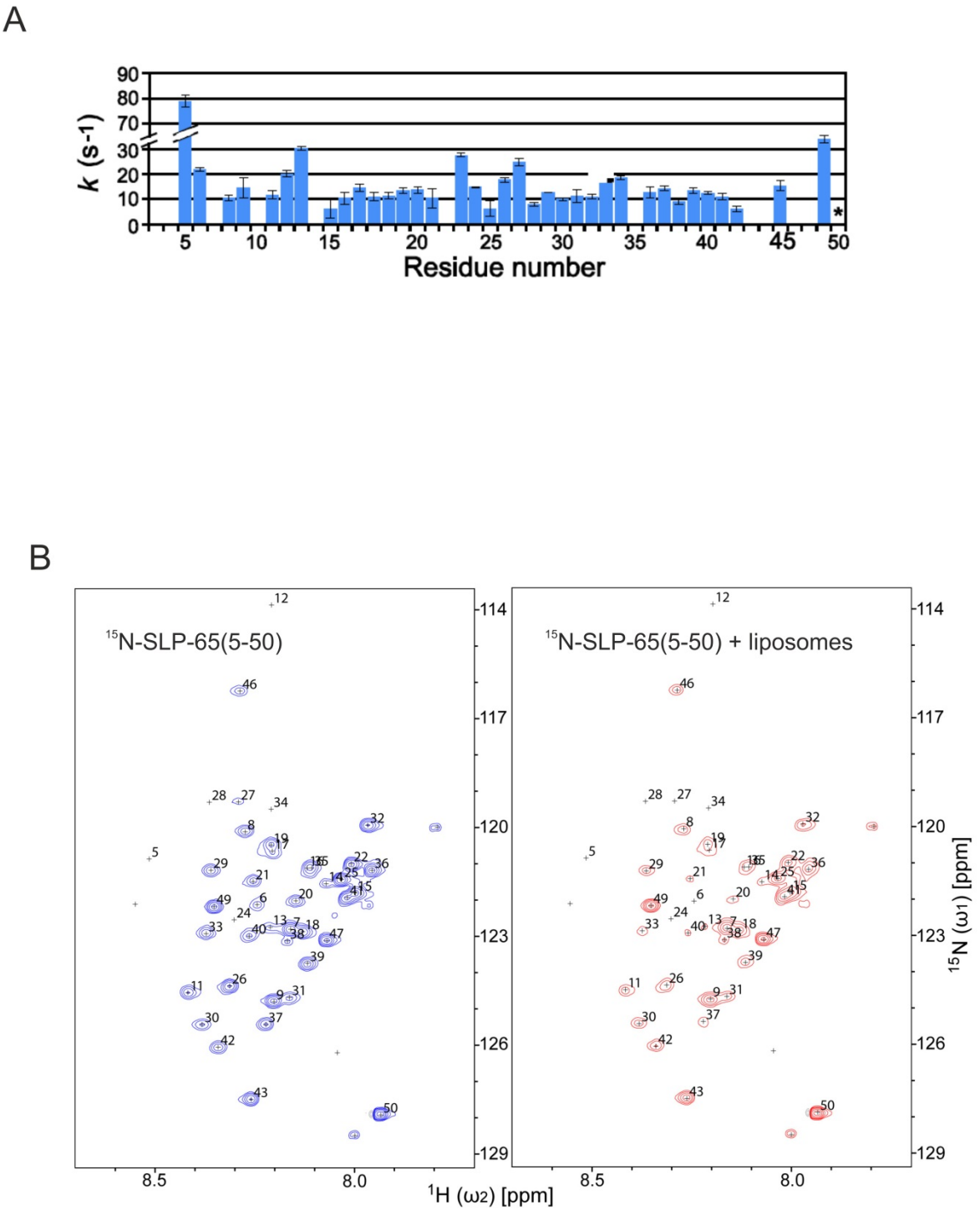

Fig. S5. The N terminus of SLP-65 is intrinsically disordered in solution and binds directly to liposomes. (**A**) Fast water-amide proton exchange rates show the solvent exposure of the polypeptide backbone as well as its lack of secondary structure. Residue R50 had an unexpectedly slow exchange rate. The exchange rates were determined by least-square fitting of the amide intensities repolarized by water to the equation $I = I_{\infty}(1\text{-}e^{-kt})$, neglecting longitudinal relaxation and partial saturation of water resonance. (**B**) ^{15}N-HSQC spectra of SLP-65(5-50) before and after the addition of liposomes (with a total lipid concentration of 10.9 mM). Both spectra were shown with the same contour level.

fig. S6

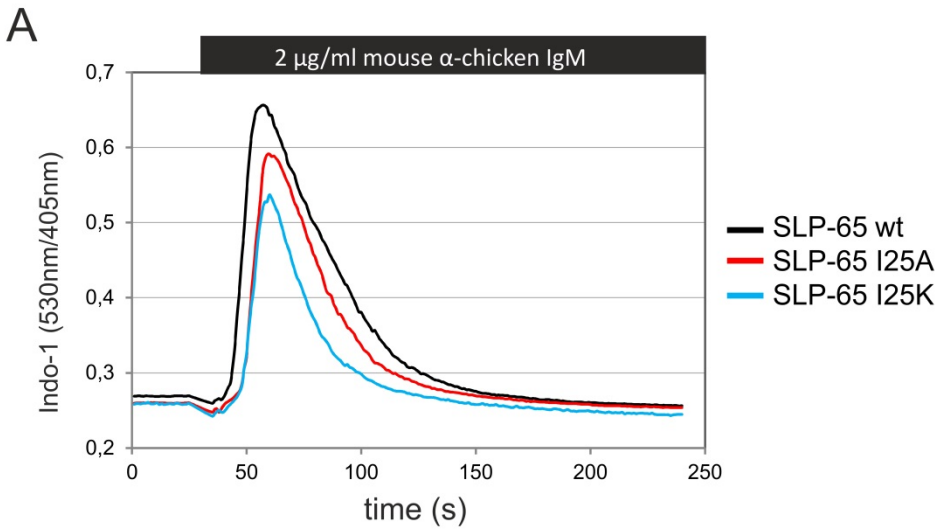

Fig. S6. Inactivation of the putative leucine zipper motif only marginally affects BCR-induced Ca^{2+} mobilization. SLP-65–deficient DT40 cells were transduced with retroviruses expressing citrine-tagged WT SLP-65 or the I25A or I25K variants of SLP-65. The cells were stimulated through the BCR with anti-chicken IgM (2 µg/ml), and Ca^{2+} flux profiles were recorded by flow cytometric analysis of cell populations that were gated for equivalent amounts of citrine-tagged proteins. Data are representative of three independent experiments.

fig. S7

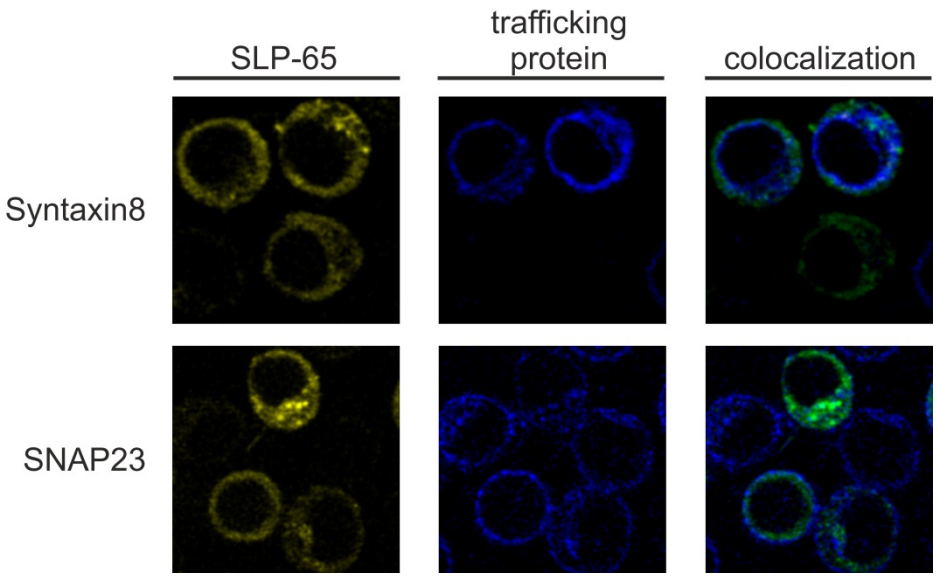

Fig. S7. Lack of colocalization between SLP-65 and syntaxin 8 and SNAP23. SLP-65-deficient DT40 cells were reconstituted with citrine-tagged SLP-65 together with cerulean-tagged versions of either syntaxin8 (top) or SNAP23 (bottom), and cells were then analyzed by confocal laser scanning microscopy. Images were processed with ImageJ software with restrictive background subtraction and Gauss filter. Citrine signals are shown in the right panels, and cerulean images are in the middle panels. In the right panel a colocalization plot is shown, which was generated with ImageJ and shows non-colocalized citrine and cerulean signals in green and blue, respectively. Colocalized signals would be indicated by a color range from gray to white depending on the degree of colocalization. Images are representative of two independent experiments.

fig. S8

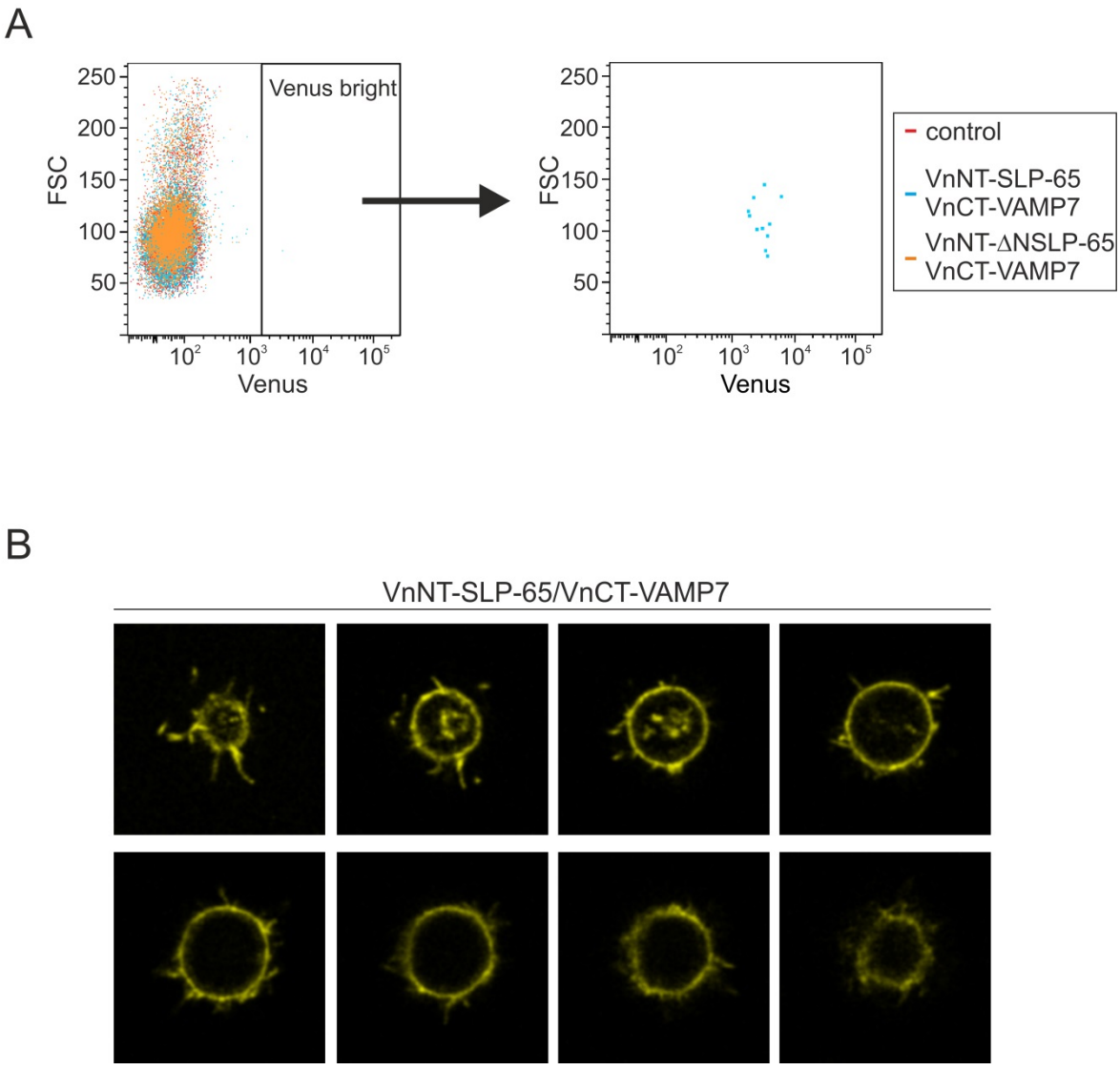

Fig. S8. N terminus–dependent attachment of SLP-65 to VAMP7-positive vesicles as revealed by bimolecular fluorescence complementation experiments. (**A**) Flow cytometric analysis of SLP-65–deficient DT40 cells that were transduced with retroviruses expressing a fusion protein between the 72 C-terminal amino acids of the fluorophore Venus and VAMP7, together with retroviruses expressing fusion proteins between the N-terminal 173 amino acids of Venus and either WT SLP-65 (blue) or the ΔN variant SLP-65 (orange). An empty vector served as a negative control (red). Cells were analyzed 72 hours after retroviral transduction. Cells found in the Venus-positive gate ("bright") are highlighted in the dot plot shown on the right. Consistent with the data shown in Fig. 3, bimolecular fluorescence complementation occurred only in transductants that produced the VAMP-Venus chimera together with the Venus chimera containing WT SLP-65, but not with the Venus chimera containing the ΔN-SLP-65 variant. (**B**) Venus-positive cells identified in (A) were further analyzed by confocal microscopy. Depicted are 8 consecutive images of a z-stack obtained from a representative cell. Data are representative of two independent experiments.

fig. S9

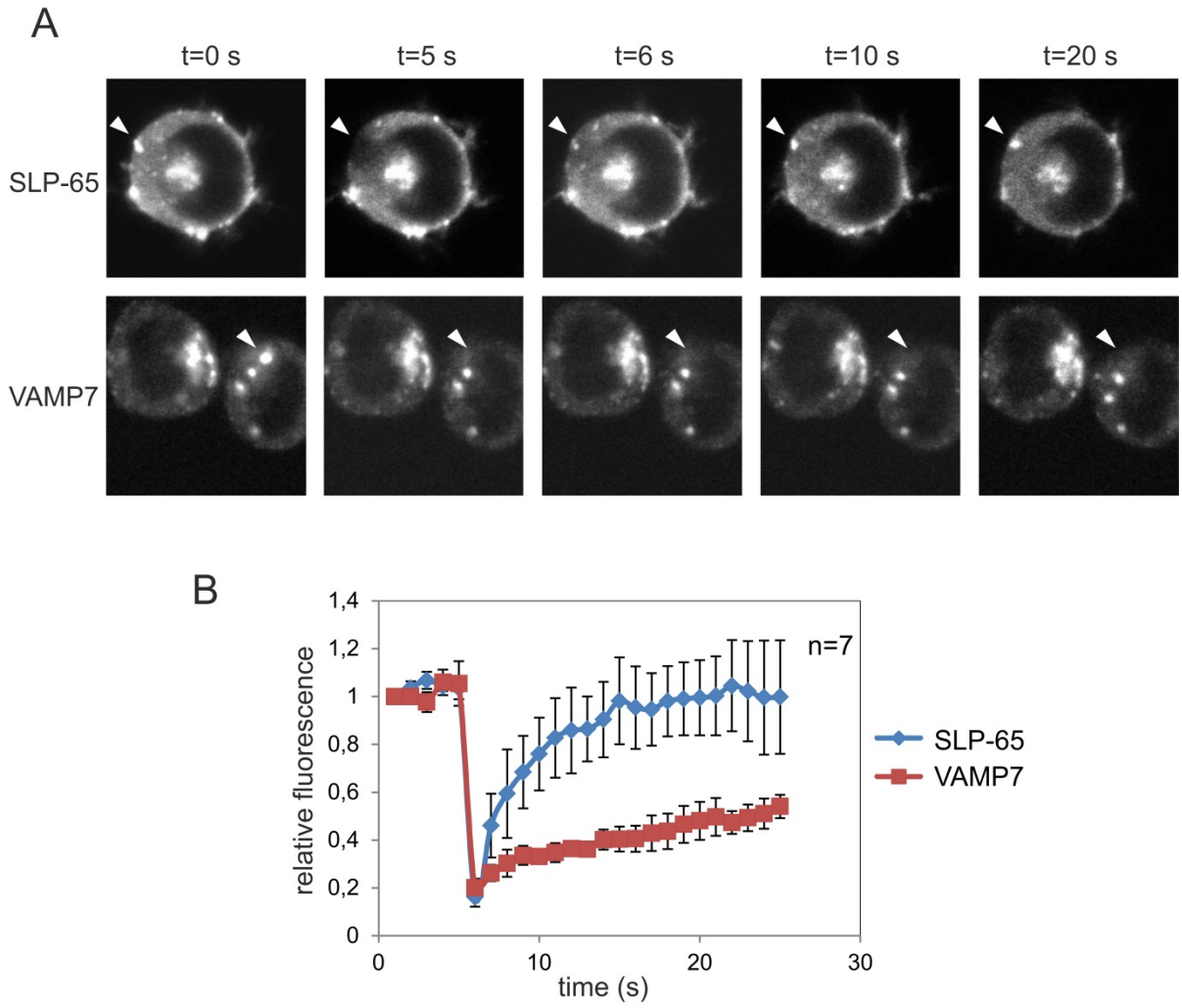

Fig. S9. The vesicle-associated and cytosolic SLP-65 pools exchange rapidly with each other. (**A**) FRAP analysis of live DT40 cell transductants expressing citrine-tagged SLP-65 (top) or cerulean-tagged VAMP7 (bottom). Representative confocal images at the indicated times of the FRAP series are shown. Photobleaching of the indicated region of interest (ROI, arrow head) was achieved with maximum laser power, and fluorescence recovery was subsequently monitored. (**B**) The fluorescence signals of seven FRAP time-lapsed series in the ROI of individual images at 25 time points (5 before, and 20 after photobleaching) were quantified for each cell type after applying background subtraction and bleaching correction with ImageJ software. Data are the normalized mean values ± SD.

fig. S10

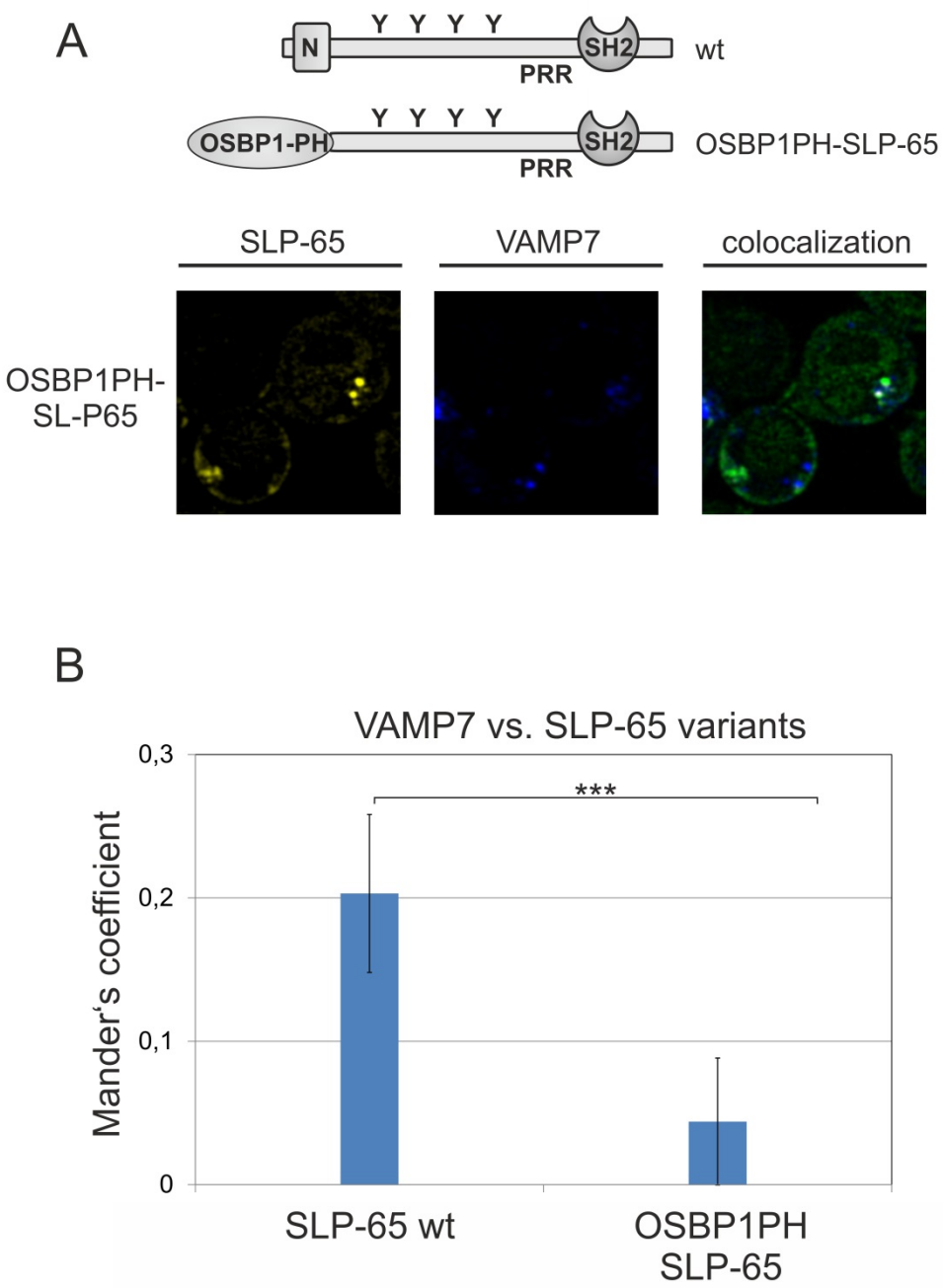

Fig. S10. The OSBP1-PH domain is insufficient to target chimeric SLP-65 protein to VAMP7-positive vesicles. (**A**) Confocal laser scanning microscopy images of SLP-65–deficient DT40 cells reconstituted with a citrine-tagged SLP-65 chimera containing the PIP_4-specific PH domain of OSBP1 instead of the N-terminal 45 amino acid residues of SLP-65, as schematically depicted. Images are of citrine and cerulean signals (left and middle panels, respectively) and of colocalization generated with ImageJ software (right panel). Non-colocalized signals are in green and blue for citrine and cerulean, respectively, whereas colocalized signals are shown in a range from gray to white, depending on the degree of colocalization. Gauss filtering was applied to all images. (**B**) Mander's coefficients for cerulean signals that colocalized with citrine signals were calculated after restrictive background subtraction for 13 z-stacks with ImageJ software. Values were compared with those of WT SLP-65, which were taken from Fig. 2B. Data are means ± SD, and statistical significance was determined by a two-tailed, unpaired t test. ***$P < 0.0001$.